Complexes of Oxygenated *trans*-Azoalkanes and Tetracyanoethylene. The Interaction of π Oxygen Dipoles with an Electron Poor Alkene

Melinda L. Greer and Silas C. Blackstock*

Department of Chemistry, University of Alabama, Tuscaloosa, Alabama 35487-0336

Received May 29, 1996[⊗]

The *N*-oxide and *N*,*N*′-dioxide (**1ao** and **1ado**) of *trans*-1,1′-azonorbornane (**1**) associate with TCNE in solution and in the solid state. The solution complexes are characterized by charge-transfer optical absorptions at λ_m 364 and 540 nm in CH_2Cl_2 for **1ao**/TCNE and **1ado**/TCNE, respectively. These complexes are weakly bound, with K_f values of 0.5−3.0 M^{-1}. Crystals of (**1ao**)$_2$/TCNE and **1ado**/TCNE are isolable, and their structures have been determined by X-ray diffraction. Local donor−acceptor (DA) interactions between the π dipolar donors and the electron poor TCNE are found. Crystals of (**1ao**)$_2$/TCNE are composed of discrete D−A−D triads in which the **1ao** oxygen approaches one of the olefinic C atoms (C_1, 2.86 Å) of TCNE more closely than the other (C_2, 3.07 Å). The O−C_1−C_2 angle is 87°, and the azooxide molecular plane lies perpendicular to the molecular plane of TCNE. **1ado**/TCNE crystals are composed of extended −D−A−D−A− strands in which both oxygen poles of the azodioxide simultaneously interact with alternate TCNE acceptors. The D−A geometry here is structurally analogous to that in the (**1ao**)$_2$/TCNE crystal. PM3 calculations of 1:1 and 1:2 *trans* HN(O)NH(O)/TCNE complexes constrained to have D−A (O−C) distances of 2.88 Å, but which are otherwise geometry optimized, reproduce the DA topology observed in the crystalline samples.

Introduction

How molecules interact at 2−3 Å (just within van der Waals contact) is an important facet of their chemistry, but one which is generally difficult to evaluate experimentally. By examining donor−acceptor (DA) complexes[1] formed between organic *N*-oxide donors and electron deficient π acceptors, such as tetracyanoethylene (TCNE), we have begun to elucidate the energetics and geometric preference of the resident weak intermolecular interactions within the 2−3 Å zone for these substrates.

Previous work has shown that oxygenated *cis*-azoalkanes derived from 2,3-diazabicyclo[2.2.2]oct-2-ene form crystalline complexes with TCNE.[2] The X-ray diffraction crystal structures of these complexes showed D−A−D triads with cyclic intermolecular atomic contacts of 2.76−3.15 Å between D and A functional groups. Because the complex geometries in these cases were correctly predicted by pericyclic reaction theory[3] (normally applied to concerted cycloaddition transition structures), these polycyclic D−A−D triads were termed "pericyclic arrays" in the solid state (see Figures 1 and 2).

The short D−A contacts and the success of pericyclic structure theory in the above cases suggest that the D−A geometries may be influenced by intermolecular orbital overlap, primarily donor HOMO−acceptor LUMO. This is consistent with Mulliken's "whole molecule" description of DA complexes.[1a] However, while electrostatic interactions and closest packing effects in crystal lattices are well documented,[4,5] the importance of orbital overlap to lattice structure is less established. We surmise that D−A orbital interactions should influence lattice structure in DA crystals when D−A partners are inside van der Waals contact. To examine this issue more closely, we are studying a series of DA crystals in which the donor HOMO topology varies (using TCNE as acceptor) in order

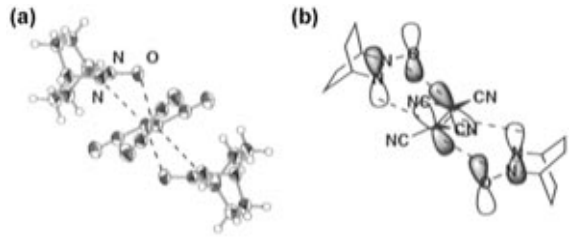

Figure 1. (a) Crystal structure of 2,3-diazabicyclo[2.2.2]oct-2-ene *N*-oxide complex with TCNE and (b) FMO diagram for a $\pi 4_s + \pi 2_s + \pi 4_s$ pericyclic array.

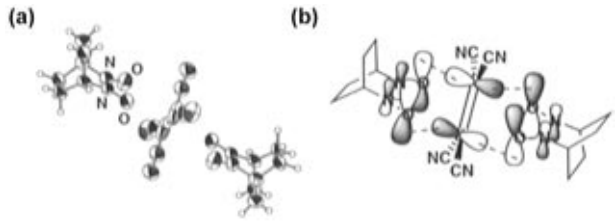

Figure 2. (a) Crystal structure of 2,3-diazabicyclo[2.2.2]oct-2-ene *N*,*N*′-dioxide complex with TCNE and (b) FMO diagram for a $\pi 6_a + \pi 2_s + \pi 6_a$ pericyclic array.

[⊗] Abstract published in *Advance ACS Abstracts,* October 15, 1996.

(1) For reviews of donor−acceptor chemistry, see: (a) Mulliken, R. S.; Person, W. B. *Molecular Complexes: A Lecture and Reprint Volume*; Wiley-Interscience: New York, 1969. (b) Hanna, M. W.; Lippert, J. L. in *Molecular Complexes*; Foster, R., Ed.; Elek Science: London, 1973; Vol. 1, Chapter 1. (c) Andrews, L. J.; Keefer, R. M. *Molecular Complexes in Organic Chemistry*; Holden-Day: San Francisco, 1964.

(2) Blackstock, S. C.; Poehling, K.; Greer, M. L. *J. Am. Chem. Soc.* **1995**, *117*, 6617.

(3) (a) Woodward, R. B.; Hoffmann, R. *The Conservation of Orbital Symmetry*; Verlag Chemie: Weinheim/Bergstr., Germany, and Academic Press: New York, 1970. (b) Zimmerman, H. E. *Acc. Chem. Res.* **1971**, *4*, 272. (c) Dewar, M. J. S. *Angew. Chem., Int. Ed. Engl.* **1971**, *10*, 761. (d) Fukui, K. *Acc. Chem. Res.* **1971**, *4*, 57.

(4) Kitaigorodskii, A. *Molecular Crystals and Molecules*; Academic Press: New York, 1973.

(5) In contrast, for an account of the general unimportance of relative dipole orientations in crystals, see: Whitesell, J. K.; Davis, R. E.; Saunders, L. L.; Wilson, R. J.; Feagins, J. P. *J. Am. Chem. Soc.* **1991**, *113*, 3267.

S0022-3263(96)00998-X CCC: $12.00

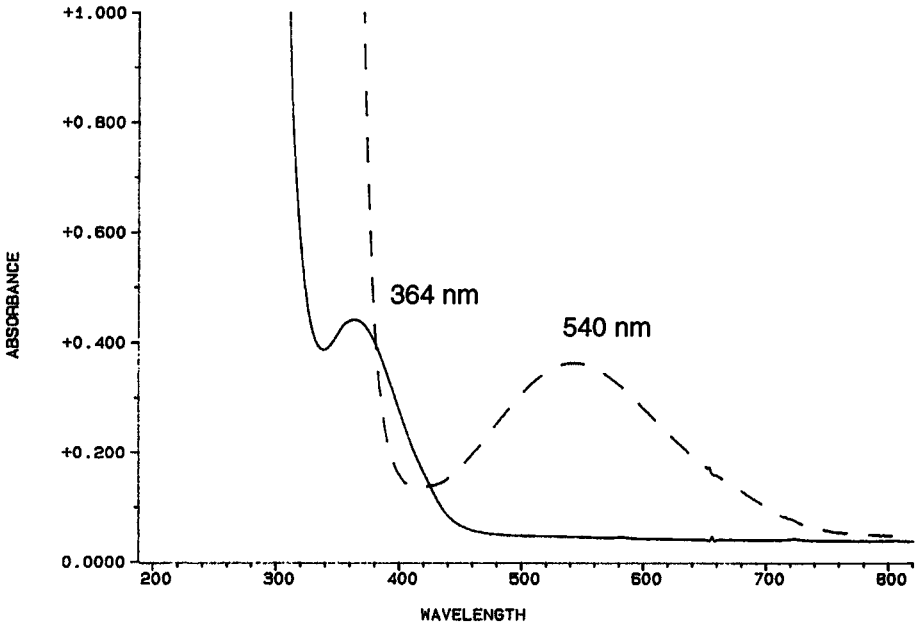

Figure 3. UV−vis spectra in CH_2Cl_2 of **1ao** (17.3 mM) and TCNE (40 mM), solid line, and **1ado** (98.4 mM) and TCNE (3.7 mM), dashed line.

to determine the relationship between component FMO topologies and the resulting D−A geometry in the crystal lattice. In the course of this work, we seek to unveil the general interaction modes of NO donors with organic olefinic acceptors in the solid state and to develop these associations as tools (or solid state synthons[6]) for crystal engineering.[7]

In this report, the effect of azoalkane stereochemistry on azooxide/TCNE and azodioxide/TCNE complexation in solution and in the crystalline solid is explored. Azooxide (**1ao**) and azodioxide (**1ado**) donors possessing

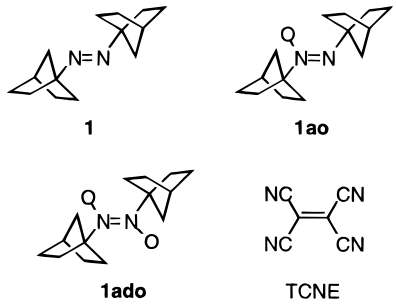

trans alkyl groups (derived from *trans*-1,1′-azonorbornane, **1**) are substrates for interaction with TCNE. The strength and structure of these D−A complexations are determined and compared to those previously observed for oxygenated *cis*-azoalkane/TCNE complexes.[2]

Results

trans-1,1′-Azonorbornane *N*-oxide (**1ao**) was prepared by *m*-CPBA oxidation of **1**, and *trans*-1,1′-azonorbornane *N*,*N*′-dioxide (**1ado**) was synthesized by *m*-CPBA oxidation of 1-aminonorbornane. In the latter case, initially formed 1-nitrosonorbornane subsequently dimerizes to give **1ado**. The azodioxide form of this molecule is favored at equilibrium in CH_2Cl_2 over its monomeric nitrosoalkane structure, making it an especially well suited *trans*-azodioxide substrate for our study.[8,9]

Solution Complexes. Mixtures of either **1ao** or **1ado** with TCNE in CH_2Cl_2 possess UV−vis absorption bands which belong to neither component of the mixtures (see Figure 3). The new bands (λ_m 364 and 540 nm for **1ao**/TCNE and **1ado**/TCNE, respectively) are assigned as charge-transfer (CT) excitations of the associated DA complexes. ^{1}H NMR spectroscopy of the DA mixtures in deuterated solvent shows that no covalent reaction occurs in either case. Benesi−Hildebrand (B−H) analysis[10] was used to estimate K_f values of complexation and the complex absorptivities (ϵ).[11] The results are shown in Tables 1, 3, and 4. Temperature dependent K_f determinations were performed to determine $\Delta H°$ and $\Delta S°$ of DA complexation. These results are given in Tables 1, 5, and 6.

Solid State Complexes. Mixed crystals of both **1ao** and **1ado** donors with TCNE have been isolated and their crystal structures determined.[12] Yellow **1ao**/TCNE prisms of D_2A stoichiometry were grown from acetonitrile/ethyl acetate at 0 °C, and purple **1ado**/TCNE crystals of 1:1 D:A stoichiometry were obtained from concentrated dichloromethane solutions. Selected distances and angles in these structures are given in Table 2. For comparison, structural parameters for crystalline **1ado** are also

(6) (a) Reddy, D. S.; Ovchinnikov, Y. E.; Shishkin, O. V.; Struchkov, Y. T.; Desiraju, G. R. *J. Am. Chem. Soc.* **1996**, *118*, 4085. (b) Reddy, D. S.; Craig, D. C.; Desiraju, G. R. *J. Am. Chem. Soc.* **1996**, *118*, 4090.

(7) For some leading reviews on crystal engineering see: (a) Desiraju, G. R. *Crystal Engineering: The Design of Organic Solids*; Elsevier: Amsterdam, 1989. (b) Whitesides, G. M.; Simanek, E. E.; Mathias, J. P.; Seto, C. T.; Chin, D. N.; Mammen, M.; Gordon, D. M. *Acc. Chem. Res.* **1995**, *28*, 37.

(8) Greer, M. L.; Sarker, H.; Mendicino, M. E.; Blackstock, S. C. *J. Am. Chem. Soc.* **1995**, *117*, 10460.

(9) For a review of azodioxides, see: Gowenlock, B. G.; Lüttke, W. *Q. Rev., Chem. Soc.* **1958**, *12*, 321.

(10) Benesi, H. A.; Hildebrand, J. H. *J. Am. Chem. Soc.* **1949**, *71*, 2703.

(11) Complex stoichiometries in solution are not known but have been assumed to be 1:1 D:A under the B−H conditions as is traditionally done. For B−H runs with [D] ≫ [A], 2:1 D:A complexation may be occurring to some extent.

(12) The authors have deposited atomic coordinates for these structures with the Cambridge Crystallographic Data Centre. The coordinates can be obtained, on request, from the Director, Cambridge Crystallographic Centre, 12 Union Road, Cambridge, CB2 1EZ, U.K.

Table 1. Spectroscopically Derived 1ao/TCNE and 1ado/TCNE Solution Complexation Constants

entry	donor/ acceptor	solvent	K_f (M^{-1}), temp (°C)	$\Delta H°$ [a] (kcal/mol)	$\Delta S°$ [a] [cal/(mol K)]
1	**1ao**/TCNE	CH_2Cl_2	0.5 ± 0.1,[b,c] 24 °C	-2.2 ± 0.3	-5.6 ± 0.9
2		CH_2Cl_2	1.4 ± 0.3,[d,e] 24 °C	-2.8 ± 0.1	-9.4 ± 0.8
3	**1ado**/TCNE	CH_2Cl_2	3.0 ± 0.4,[c,f] 20 °C	-1.3 ± 0.01	-6.9 ± 0.2
4		CH_2Cl_2	1.3 ± 0.03,[e,g] 20 °C	-1.3 ± 0.01	-5.3 ± 0.05
5		CH_3CN	1.6 ± 0.1,[c,g] 24 °C	-3.3 ± 0.1	-11.8 ± 0.1

[a] Determined at non-B−H concentrations using ϵ from B−H study in corresponding row. Values are the average of analyses at same wavelengths as B−H study. [b] Average of three runs analyzed at λ 344, 364, 394, and 410 nm. [c] B−H analysis with [A] ≫ [D]. [d] Average of analyses at λ 410, 420, and 430 nm from a single run. [e] B−H analysis with [D] ≫ [A]. [f] Average of three runs analyzed at λ 500, 520, 540, and 550 nm. [g] Average of analyses at λ 500, 520, 540, and 550 nm from a single run.

Table 2. Selected Distances and Angles from $(1ao)_2$/TCNE, (1ado)TCNE, and 1ado X-ray Crystal Structures

	$(1ao)_2$/TCNE[a]	**1ado**/TCNE	**1ado**[b]
	Bond Lengths (Å)		
N−O	1.29(5), 1.29(4)	1.272(3)	1.269(4)
N−N	1.23(5), 1.25(4)	1.308(4)	1.308(6)
N−C	1.52(5), 1.51(4)[c] 1.57(5), 1.54(4)[d]	1.492(4)	1.483(5)
TCNE			
CN	1.11(1)[e]	1.119(5)[f]	
C−C	1.46(1)[e]	1.455(6)[f]	
C=C	1.27(1)	1.285(8)	
	Bond Angles (deg)		
ONN	126(7), 124(5)	120.5(3)	120.1(4)
ONC	126(2), 128(2)	121.0(2)	120.7(3)
CNN	109(7), 109(5)[g] 108(7), 111(5)[h]	118.6(3)	119.2(4)
ONNO		180	180
CNNC	179(1), 179(2)	180	180
ONNC	6(4), 4(3)	-0.4(5)	0
	Intermolecular Contacts (Å)		
$O-C_1$[i]	2.85(1), 2.86(1)	2.875(4)	
$O-C_2$[j]	3.08(1), 3.05(1)	3.135(4)	
	Intermolecular Angles (deg)		
$O-C_1C_2$	88.0, 86.4	89.5	
$NO-C_1$	162.5, 161.4	163.7	
$NO-C_1C_2$	88.2, 99.6	83.7	
$O-C_1C_2$-O′	178.1	180.0	

[a] Bond lengths and angles for both azooxide fragments in the asymmetric unit listed. Each value listed is an average of the two azooxide orientations used to fit disorder (see text). [b] Reference 8. [c] Geminal to NO. [d] Vicinal to NO. [e] Average of four values. [f] Average of two values. [g] CN(O)N. [h] CNN(O). [i] Oxygen to closest TCNE double bond carbon. [j] Oxygen to farthest TCNE double bond carbon.

included. To date, crystals of **1ao** suitable for X-ray analysis have not been obtained.

$(1ao)_2$/TCNE Crystals. By X-ray diffraction, a pale yellow $(\mathbf{1ao})_2$/TCNE crystal is found to contain discrete D−A−D triads as illustrated in Figures 4 and 5. In these triads, **1ao** donors approach opposite faces of the TCNE π system via the oxygen end of the azooxide dipole. Each oxygen atom is closer to one TCNE olefinic carbon (C_1, 2.86 Å) than to the other (C_2, 3.07 Å). The $O-C_1-C_2$ angle is 87°, and the triads possess nominal, although not crystallographic, inversion symmetry about the sandwiched TCNE acceptor. The D−A topology is such that the NNO molecular plane of the donor aligns perpendicular to the TCNE molecular plane.

Disorder of the donor group (as shown below) in this crystal is observed and accounts for the elevated *R*-value of 8.5% for the structure determination. Two orientations of the azooxide nitrogens (as shown) were used in a 50:50 weighting scheme for structure refinement. Although the donor nitrogens show in-plane disorder, their attached groups, the oxide oxygen and 1-norbornyl substituents, nearly superimpose in the two orientations and thus remain essentially ordered in the lattice. Despite the disorder in the $(\mathbf{1ao})_2$/TCNE crystal, the unique D−A

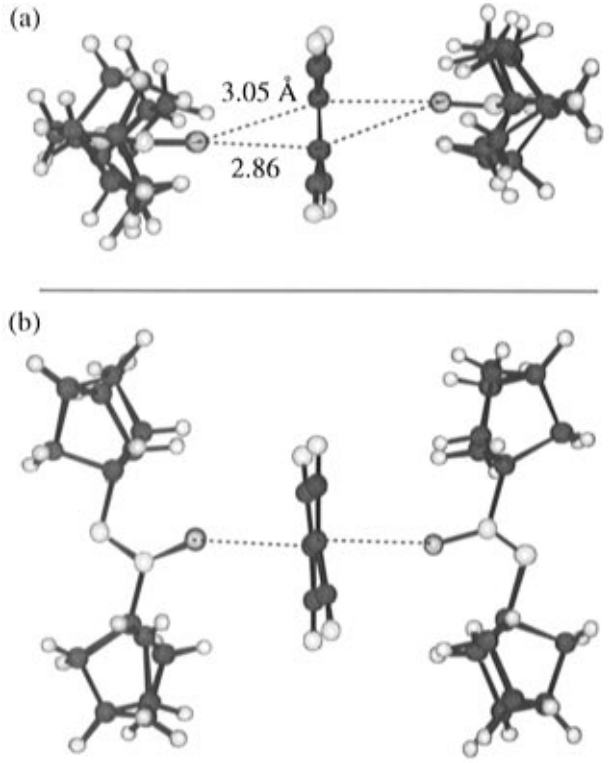

Figure 4. 1ao−TCNE−**1ao** triad within the $(\mathbf{1ao})_2$/TCNE crystal.

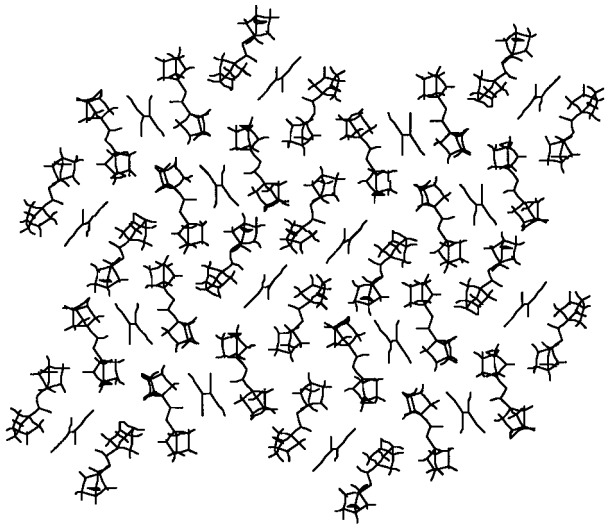

Figure 5. Partial packing diagram for the $(\mathbf{1ao})_2$/TCNE crystal.

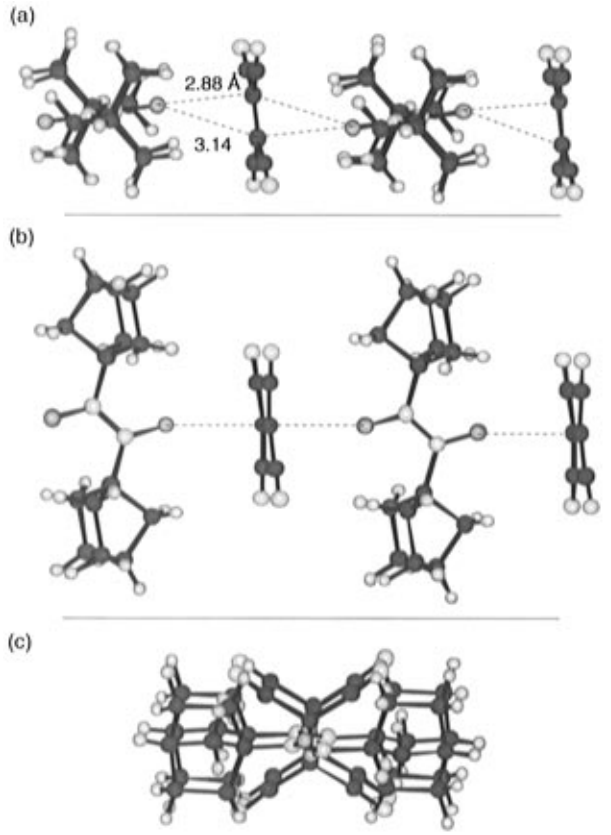

Figure 6. −D−A−D−A− strand in the **1ado**/TCNE crystal: (a) side view, (b) orthogonal side view, and (c) end view, along strand axis.

topology in this complex remains well-resolved.

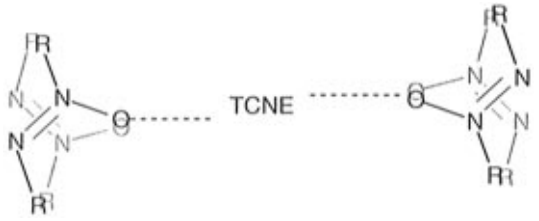

1ado/TCNE Crystals. The X-ray diffraction structure of a **1ado**/TCNE crystal shows the presence of extended −D−A−D−A− strands, made possible because the azodioxide donor contains two, *trans*-disposed oxygen donor sites, both of which interact with acceptor molecules (see Figure 6). The discrete intrastrand D−A associations are geometrically quite similar to those observed in the (**1ao**)$_2$/TCNE triads. Figure 7 provides a partial packing diagram of the **1ado**/TCNE crystal.

The (D−A)$_n$ strands of the **1ado**/TCNE solid run along the crystallographic *a*-axis with a repeat distance of 9.204 Å, the *a* cell length. Each strand has six nearest neighbors, but because of inversion symmetry, there are only three unique strand-to-strand interactions, which we label *b*, *c*, and *bc* according to the cell directions along which the interactions occur (*bc* being the diagonal of the *bc* cell face). Normal axis-to-axis interstrand distances are given in Figure 8 along with lateral views (orthogonal to the strand axis) of the three unique strand-to-strand interactions. The closest interstrand contacts are between H atoms of donor norbornyl groups at ∼3 Å.

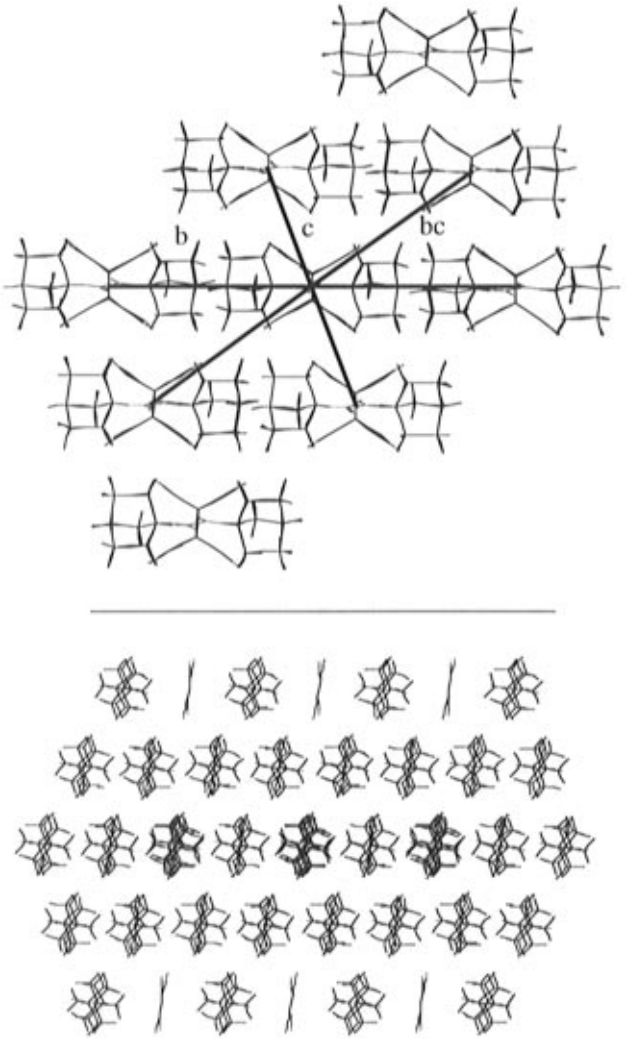

Figure 7. Partial packing diagram for the **1ado**/TCNE crystal showing parallel (D−A)$_n$ strands: above, viewed down strand axis with nearest strand-to-strand interactions marked; below, viewed perpendicular to strand axis.

Discussion

The *trans*-azo stereochemistry of azooxides **1ao** and **1ado** would appear to preclude the formation of pericyclic arrays with TCNE as previously observed for oxygenated *cis*-azoalkanes.[2] We find that these donors do associate with TCNE in solution and that a new azooxide/TCNE and azodioxide/TCNE complexation scheme results in the solid state.

Solution Complexes. Spectroscopically determined complex formation constants, K_f, for association of **1ao** and **1ado** with TCNE are low, 0.5−3.0 M^{-1}, and small negative entropies (−5 to −12 eu) and enthalpies (−1 to −3 kcal mol^{-1}) of complexation are observed (Table 1). While the latter quantities have the expected signs, their magnitudes are less negative than anticipated ($\Delta S°$ values of −15 to −30 eu are expected for ordered 1:1 associations). It may be that the B−H analysis is underestimating $\Delta H°$ and $\Delta S°$ magnitudes in these cases. In other work,[13] Herndon and co-workers showed that $\Delta H°$ and $\Delta S°$ determined calorimetrically for a set of TCNE complexes of alkylbenzene donors were consis-

(13) (a) Herndon, W. C.; Feuer, J.; Mitchell, R. E. *J. Chem. Soc., Chem. Commun.* **1971**, 435. (b) Herndon, W. C.; Feuer, J.; Mitchell, R. E. *Anal. Calorim.* **1974**, *3*, 249.

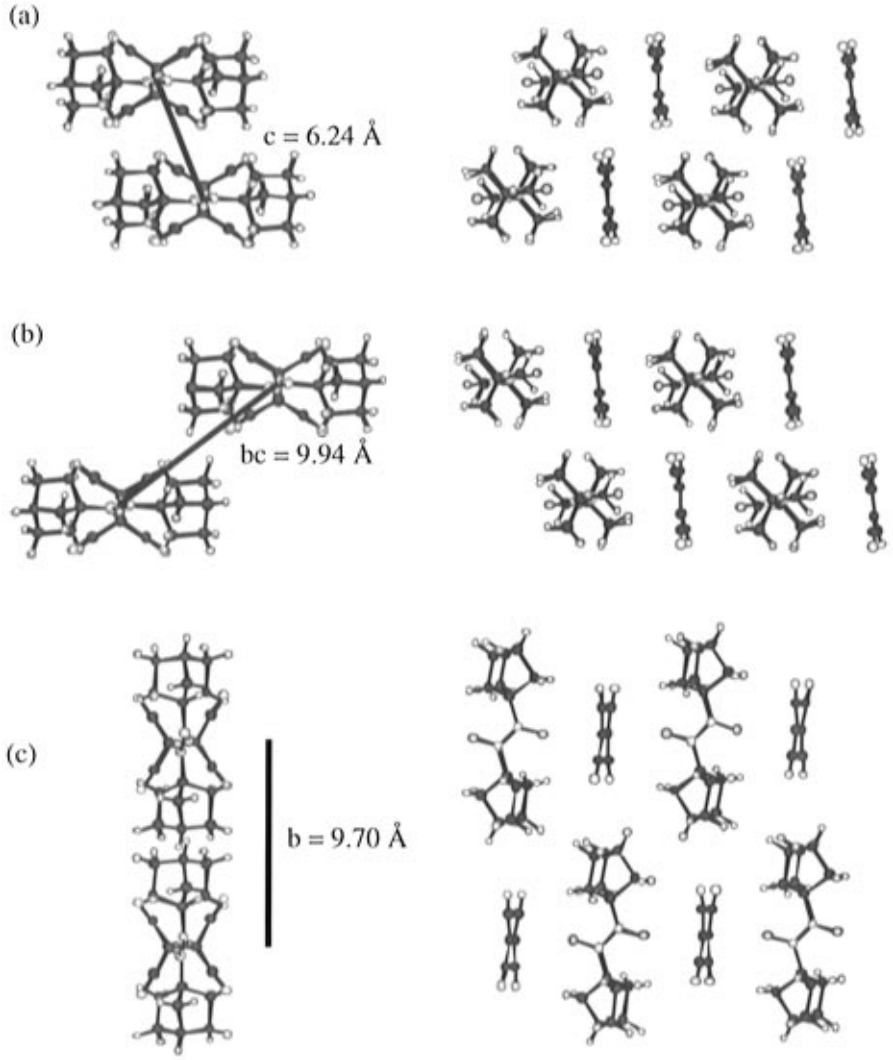

Figure 8. End (left) and side (right) views of interstrand contacts of (a) type *c*, (b) type *bc*, and (c) type *b*.

tently more negative than those found spectroscopically.[14] Generally speaking, the B−H analysis is known to be rather inaccurate for weakly bound complexes,[15] and we expect that our measurements suffer some of the typical problems associated with this treatment, which include spectral interference from contact CT absorptions among other things. One indication of internal inconsistency of the analyses is that K_f values determined at multiple CT wavelengths in a single B−H analysis vary considerably (see Tables 3 and 4). Furthermore, the use of B−H-derived ϵ values under non-B−H conditions, as employed to determine the temperature dependence of K_f, reveals significant discrepancies in K_f values determined at the different concentration regimes of these experiments.[16] Errors of this sort associated with the spectroscopic analyses of DA complexes have been previously discussed[17] and are thought to arise from oversimplified assumptions about complex stoichiometry, complex structure (and the singularity of such), and substrate activities which may not be constant across large concentration ranges. Calorimetric analyses of the azooxide/TCNE and azodioxide/TCNE associations would probably yield more accurate thermodynamic data and are planned. For now, we conclude only that, at 25 °C, the **1ado**/TCNE and **1ao**/TCNE solution complexations are nearly thermoneutral, with entropy costs of complexation counterbalanced by enthalpy gains.

Of the two donors studied here, **1ado** is the stronger based on its lower energy TCNE complex CT absorption (λ_{mCT} 540 nm, compared to 360 nm for **1ao**/TCNE) and its easier anodic oxidation ($E^{\circ\prime}$ = 1.5 V vs SCE for **1ado** compared to E_{pa} > 2.2 V for **1ao**, determined by cyclic voltammetry). The same trend in donor strength is observed in the CT absorptions of oxygenated *cis*-azoalkanes[2] as would also be predicted from the relative gas phase ionization potentials of *cis*-azo mono- and dioxides.[18] Despite the large difference in the donor strengths of azo mono- and dioxides, the **1ao** and **1ado** abilities to complex TCNE appear surprisingly similar as assessed by the, albeit crude, data of Table 1.

(14) K_f, $\Delta H°$, and $\Delta S°$ for TCNE/toluene complexation in CH_2Cl_2 at 22 °C were found to be 0.234 M^{-1}, −2.96 kcal mol^{-1}, and −12.8 cal mol^{-1} deg^{-1}, respectively, by spectroscopic analysis (Bolles, T. F.; Drago, R. S. *J. Am. Chem. Soc.* **1965**, *87*, 5015). The same quantities measured calorimetrically by Herndon et al. at 25 °C were 0.132 M^{-1}, −7.88 kcal mol^{-1}, and −30.2 cal mol^{-1} deg^{-1} (ref 13a).

(15) See: Foster, R. In *Molecular Complexes*; Foster, R., Ed.; Elek Science: London, 1974; Vol. 2, Chapter 3.

(16) Because of limited solubilities, it was necessary to perform the temperature dependent K_f analyses under non-B−H conditions.

(17) See: Tamres, M; Strong, R. L. in *Molecular Association*, Foster, R., Ed.; Academic Press: New York, 1979; Vol. 2, Chapter 5.

(18) (a) Gilbert, K. *J. Org. Chem.* **1977**, *42*, 609. (b) Bünzuli, J.-C. G.; Olsen, H.; Snyder, J. P. *J. Org. Chem.* **1977**, *42*, 614.

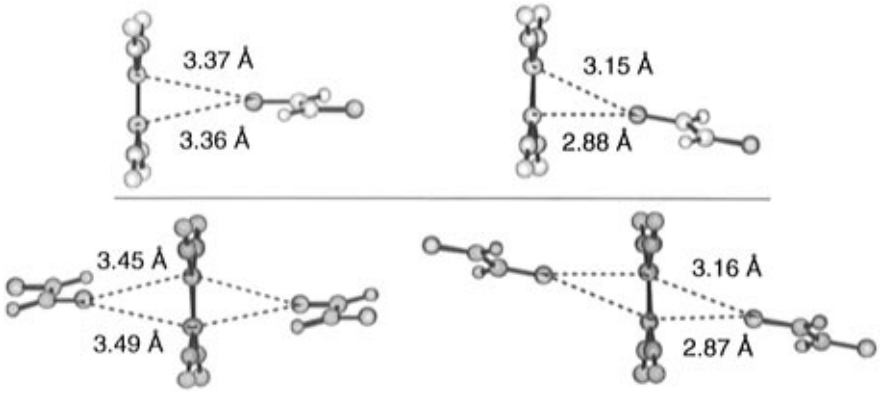

Figure 9. PM3-calculated azodioxide−TCNE diad (top) and azodioxide−TCNE−azodioxide triad (bottom) with C_i symmetry. Left complexes are fully optimized and right structures are optimized with one C−O distance constrained as indicated.

Crystalline Complexes.[19] The mixed **1ao**/TCNE and **1ado**/TCNE crystals are highly colored and are composed of constituent D−A pairs positioned inside of van der Waals contact (vide infra) of each other in the respective crystal lattices. These features indicate the presence of specific D−A intermolecular interactions in the DA crystals. Thus, we view these crystals as conglomerates of *associated* donors and acceptors and suggest that the D−A functional group interactions strongly influence the assembly and ultimate structure of the two-component lattice. As has been pointed out by Kitaigorodskii,[20] the formation of mixed DA crystal lattices does not necessarily imply specific intermolecular interactions between the components. Mixed crystals can result from a variety of factors which may stabilize the lattice, including shape-selective closest packing of unlike molecules, dipolar interactions between polar constituents, and weak bonding interactions between molecular components. In the cases of **1ao**/TCNE and **1ado**/TCNE crystals, however, both the molecular periodicity and the close intermolecular contacts strongly suggest the latter factor operates, although all of the above phenomena are likely at play to some extent. Of course, the weakly bonding D−A interactions facilitate crystal packing efficiency despite exerting a certain degree of associated molecular ordering in the lattice.

Complex Geometries. The anisotropy of the local D−A interactions between the oxide oxygen(s) and the TCNE double bond carbons which creates the triads in (**1ao**)$_2$/TCNE and the extended strands in **1ado**/TCNE is strikingly similar in these two crystals. The most significant features of these complexations are intermolecular distance and topology. The D−A O−C contacts of 2.86−2.88 and 3.05−3.14 Å are less than the van der Waals O−C distance of 3.22 Å.[21] Thus, we may reasonably assume that some DA orbital overlap occurs in these complexes. The observed complex topologies are consistent with p−π* FMO interactions ($\omega_a + \pi_s$ overlap) between the azooxide oxygen p orbital of the NO dipole and the TCNE π* orbital. One might expect that an optimum p−π* HOMO−LUMO interaction would occur when the azooxide oxygen is equidistant from the two olefinic carbons of TCNE to align the FMO nodal planes, giving a $\omega 2_a + \pi 2_s$ quasi-pericyclic array. The observed structure indeed aligns the azooxide oxygen p orbital axis with the central CC TCNE bond but holds the donor oxygen atom closer to one of the TCNE carbons than the other, with a nearly 90° O−CC angle. Whether this arrangement optimizes HOMO−LUMO overlap or perhaps results from compression of the complex in the lattice remains unknown.[22] To gain a prediction of the preferred azodioxide/TCNE interaction in the absence of medium influences, computational modeling of the interaction has been employed.

Computational Modeling. To model the D−A electronic interactions of interest here, semi-empirical PM3 calculations[23] of *t*-RN(O)NR(O)−TCNE and of *t*-RN(O)-NR(O)−TCNE−*t*-RN(O)NR(O) assemblies were performed with $R = CH_3$, H. Figure 9 displays the resulting optimized D−A dyad and C_i D−A−D triad structures (employing C_s donor and acceptor structures). In one case, full optimization of the complex geometry (including intermolecular contacts) was performed, and in another case, complexes were constrained to have one O−C distance of 2.87 or 2.88 Å (as observed in the crystals) but were otherwise geometry optimized. The resultant structures have nearly the same D−A topology found in the (**1ao**)$_2$/TCNE and **1ado**/TCNE crystals. These results suggest that the geometry observed in the complex crystals is the electronically preferred one. Furthermore, the calculations suggest that one azodioxide donor complexes TCNE in much the same way as do two. Calculated complexation enthalpies are ∼2.5 kcal mol^{-1} for D−A and ∼5.0 kcal mol^{-1} for D−A−D formation (see Experimental Section for details). As expected, geometrical preferences within these complexes are very slight with lateral or vertical motions of the donor about TCNE costing 1.0−3.0 kcal mol^{-1} and angular reorientations of the donor costing about 0.2−0.5 kcal mol^{-1}. Of course, the reliability of calculated shallow potential energy surfaces is marginal at best. Nevertheless, we are intrigued that PM3 structural predictions mirror so well the observed crystal structures. Higher level ab initio computation of these functional group interactions is planned.

(19) For general reviews of organic DA crystal structures, see: (a) Herbstein, F. H. *Perspect. Struct. Chem.* **1971**, *4*, 166. (b) Prout, C. K.; Kamenar, B. in *Molecular Complexes*; Foster, R., Ed.; Elek Science: London, 1973; Vol. 1, Chapter 3. (c) Soos, Z. G.; Klein, D. J. In *Molecular Association*; Foster, R., Ed.; Academic Press: New York, 1975; Vol. 1, Chapter 1. (d) Foster, R. *Organic Charge-Transfer Complexes;* Academic Press: New York, 1969; Chapter 8.

(20) Kitaigorodskii, A. I. *Mixed Crystals*; Springer-Verlag: Berlin, 1984.

(21) (a) Bondi, A. *J. Phys. Chem.* **1964**, *68*, 441. (b) Rowland, R. S.; Taylor, R. *J. Phys. Chem.* **1996**, *100*, 7384.

(22) It is tempting to interpret the D−A geometries observed in these crystals as being those energetically preferred independent of medium. However, close-packing and/or crystal field effects in the lattice may surely influence the local D−A structures. More examples of mixed crystal structures involving similar functional group interactions are needed before the generality of the π oxygen anion−TCNE interactions observed here can be assessed.

(23) Stewart, J. J. P. *J. Comput. Chem.* **1989**, *10*, 209.

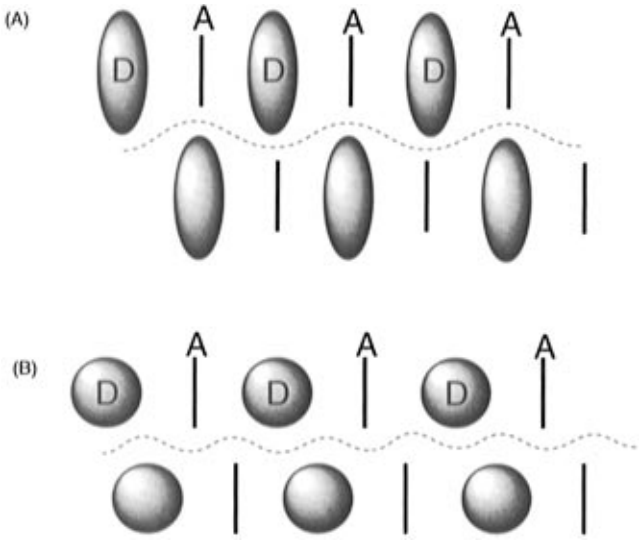

Figure 10. Interlocking of beaded −D−A−D−A− strands (a) along *b* direction and (b) along *c* and *bc* directions.

Interstrand Interactions. The **1ado**/TCNE structure contains parallel −D−A−D−A− strands whose interstrand arrangement in the crystal lattice is responsible for second- and third-dimensional ordering in the composite. At issue is interstrand slippage (or the phase relation between strands) in the three unique strand-to-strand orientations. The interstrand structure appears to be dictated by shape-selective closest packing. Figure 10 illustrates how the strand contours mesh in the crystal lattice. Whether interstrand dipolar interactions are a factor in this structure is not known. Interstrand contacts are larger than the sum of atomic van der Waals radii, suggesting that chemically specific strand-to-strand interactions are not present.

Summary

Oxygenated *trans*-azoalkanes form DA complexes with TCNE. Complex formation in solution is observed by the presence of new bands in the UV−vis spectrum in accord with Mulliken's theory.[1a] The **1ao**/TCNE and **1ado**/TCNE pairs are classified as weakly bound complexes on the basis of the magnitude of their formation constants (0.5−3.0 M^{-1}) in solution. Crystals of (**1ao**)$_2$/TCNE and **1ado**/TCNE are composed of interacting D−A arrays. Almost identical D−A interactions are found in both types of crystals, with the donor oxygen approaching (2.86−2.88 Å) one of the C atoms of the TCNE double bond more closely than the other (3.04−3.14 Å), and the azooxide NNO molecular plane aligning perpendicular to that of the TCNE acceptor. The (**1ao**)$_2$/TCNE crystal contains D−A−D triads while **1ado**/TCNE crystals are composed of parallel extended −D−A−D−A− strands. Semiempirical PM3 calculations of *t*-HN(O)NH(O) and *t*-MeN(O)NMe(O) donors with TCNE constrained to have one O−C distance of 2.88 Å, but otherwise geometry optimized, reproduce the complex topology observed in the crystalline samples.

Experimental Section

General Methods. C, H, N analyses were obtained from Atlantic Microlab Inc., Norcross, GA. DEPT NMR experiments were used to establish the hydrogen multiplicity of the ^{13}C NMR signals. Crystallographic measurements were made on a Rigaku AFC6S diffractometer with graphite-monochromated Cu Kα radiation at 20 °C, and TEXSAN software was used for crystal structure solution and refinement.

Acetonitrile (HPLC grade) was refluxed over and then distilled from P_2O_5 before use. Dichloromethane was stirred overnight over concd H_2SO_4, decanted, washed with aqueous $NaHCO_3$ and water, and then refluxed and distilled from CaH_2. Tetracyanoethylene was purified by repetitive sublimation through a bed of activated charcoal.

***trans*-1,1′-Azonorbornane *N,N*′-Dioxide (1ado).** Azodioxide **1ado** was prepared by *m*-CPBA oxidation of 1-aminonorbornane[24a] as previously described.[8]

***trans*-1,1′-Azonorbornane (1).** The synthesis of **1** has been previously reported.[24] We prepared **1** as follows. Dry *trans*-1,1′-azonorbornane *N,N*′-dioxide (**1ado**) (0.4926 g, 0.00198 mol) in 15 mL of CH_2Cl_2 was placed into a moisture-free flask under an argon atmosphere, and Si_2Cl_6 (0.850 mL, 0.00493 mol) was added slowly via syringe through a septum with stirring. The resulting mixture was stirred under argon in the dark overnight to yield a pale yellow solution. After addition of 1 M NaOH (100 mL), the mixture was extracted with CH_2Cl_2 (6 × 25 mL). The combined organic layers were dried over anhyd K_2CO_3 and evaporated *in vacuo* to yield crude **1** as a pale yellow solid (0.402 g, 93%), which was further purified by recrystallization from ether/methanol: mp 164−165 °C (lit.[24a] mp 164 °C).

***trans*-1,1′-Azonorbornane *N*-Oxide (1ao).** *trans*-1,1′-Azonorbornane (**1**) (122.2 mg, 0.5606 mmol) was dissolved in CH_2Cl_2 (2 mL) in a small flask and treated with *m*-CPBA (80%, 120.7 mg, 0.5600 mmol). The mixture was stirred for 10 min, diluted with ∼5 mL of CH_2Cl_2, and then extracted with 10% $Na_2S_2O_3$ (2 × 5 mL), 10% Na_2CO_3 (2 × 5 mL), and H_2O (2 × 5 mL). The organic layer was dried over anhyd K_2CO_3 and evaporated *in vacuo* to give **1ao** as an off-white solid (91.0 mg, 70%), which was purified by crystallization from CH_3CN: mp 173−175 °C; ^{1}H NMR (300 MHz, $CDCl_3$) δ 1.33−1.59 (m, 6H), 1.66 (br s, 4H), 1.86 (br s, 6H), 1.92−2.08 (m, 4H), 2.12 (m, 1H), 2.23 (m, 1H); ^{13}C NMR (360 MHz, C_3D_6O) δ 30.16 (CH_2), 30.22 (CH_2), 30.35 (CH_2), 34.69 (CH2), 35.27 (CH), 35.89 (CH), 42.39 (CH_2), 42.86 (CH_2), 71.68 (C), 86.21 (C); IR (KBr) 2955 (s), 2870 (s), 2359 (w), 1481 (s), 1316 (m) cm^{-1}; MS (EI, *m*/*z*) 234 (9), 217 (100), 205 (60), 95 (92), 67 (67). Anal. Calcd for $C_{14}H_{22}N_2O$: C, 71.79; H, 9.40; N, 11.97; O, 6.84. Found: C, 71.80; H, 9.40; N, 11.99.

Determination of Formation Constants. In a typical run, a 2-mL aliquot of a standard solution of donor was transferred to a 1-cm precision quartz cell containing a magnetic stir bar. Successive additions of preweighed amounts of TCNE to the solution were followed by thorough stirring.[25] A UV−vis spectrum was taken after each addition. Base-line absorption at 800 nm was subtracted from the absorbance at the wavelength of interest to correct for any base-line drift in the analyses.[26] Spectra of the donor and acceptor at their highest concentration were always measured to ensure that there were no absorptions from these materials in the CT band region of the spectrum of the mixed samples used in the analyses. The temperature of the solutions was monitored, and the K_f was determined according to the Benesi−Hildebrand method.[10] Multiple runs were performed in some cases to determine reproducibility and calculate standard deviations for ϵ and K_f. In addition, K_f determinations at several different λ_{CT} values within a run were performed to evaluate the internal consistency of the method. Some representative data for each complex are shown in Tables 3 and 4.

Determination of $\Delta H°$ and $\Delta S°$ of Complex Formation. A representative procedure follows. To a 1-cm precision quartz cell equipped with a stirring bar was added 2 mL of the DA

(24) (a) Golzke, V.; Groeger, F.; Oberlinner, A.; Rüchardt, C. *Nouv. J. Chim.* **1978**, *2*, 169. (b) Schmittel, M.; Rüchardt, C. *J. Am. Chem. Soc.* **1987**, *109*, 2750. (c) Neuman, R. C., Jr.; Grow, R. H.; Binegar, G. A.; Gunderson, H. J. *J. Org. Chem.* **1990**, *55*, 2682.

(25) The concentration ranges employed have been optimized to maximize CT absorption changes and the [A]/[D] ratio range (10−40 used, limited by component solubilities) to afford the most accurate B−H analyses possible.

(26) These difference absorption values (i.e., $A_{500-800}$) are reported in Tables 3−6 and Tables S1−S10 of the Supporting Information.

Table 3. Data from a Benesi−Hildebrand Study of 1ao/TCNE in CH_2Cl_2 at 24 °C[a]

1ao (mM)	TCNE (mM)	$A_{344-800}$	$A_{364-800}$	$A_{394-800}$	$A_{410-800}$
2.31	23.9	0.0419	0.0428	0.0353	0.0261
2.31	43.0	0.0753	0.0736	0.0581	0.0414
2.31	62.5	0.0993	0.1023	0.0800	0.0563
2.31	80.9	0.1251	0.1319	0.1013	0.0711
2.31	101.2	0.1531	0.1653	0.1279	0.0901
ϵ		344	444	209	114
K_f		0.43	0.55	0.31	0.22
r^2		0.998	0.999	0.998	0.995

[a] Data used to calculate values for entry 1, Table 1.

Table 4. Data from a Benesi−Hildebrand Study of 1ado/TCNE in CH_2Cl_2 at 20 °C[a]

1ado (mM)	TCNE (mM)	$A_{500-800}$	$A_{520-800}$	$A_{540-800}$	$A_{550-800}$
2.40	34.0	0.0648	0.0742	0.0771	0.0768
2.40	50.4	0.0942	0.1077	0.1126	0.1119
2.40	67.6	0.1279	0.1452	0.1519	0.1512
2.40	86.3	0.1626	0.1841	0.1927	0.1915
ϵ		2996	1836	3006	2622
K_f		3.75	1.99	3.15	2.76
r^2		1.000	1.000	1.000	1.000

[a] Data used to calculate values for entry 3, Table 1.

mixture in CH_2Cl_2. A UV−vis spectrum of the solution was taken at various temperatures (after temperature equilibration with stirring) over a range of at least 39 °C. K_f values were determined at each temperature using ϵ values from the Benesi−Hildebrand studies. $\Delta H°$ and $\Delta S°$ were then extracted from a plot of ln K_f vs $1/[T(K)]$. $\Delta H°$ and $\Delta S°$ were calculated at several λ_{CT} values within a run in order to evaluate the internal consistency of the method. Errors resulting from variation of ϵ are within the errors determined from analysis at various λ_{CT} values. Representative data are shown in Tables 5 and 6.

Crystallization of (1ao)$_2$/TCNE. 1ao (13.4 mg, 0.0573 mmol) and TCNE (3.7 mg, 0.0289 mmol) were dissolved in a minimal amount of CH_3CN/ethyl acetate (1:1). The resulting pale yellow solution was cooled to −20 °C. After several days, pale yellow-orange crystals formed: IR (KBr) 2954 (s), 2872 (s), 2256 (w), 2221 (w), 1485 (s) cm^{-1}.

Crystallization of 1ado/TCNE. 1ado (6.8 mg, 0.0272 mmol) and TCNE (3.7 mg, 0.0289 mmol) were mixed in 0.25 mL of CH_2Cl_2 to give a deep purple solution. Upon slow evaporation of the solvent at room temperature, a mixture of dark purple complex crystals and colorless crystals of TCNE and **1ado** formed. Purple crystals: mp 160−170 °C sublimed; IR (KBr) 2955 (m), 2878 (m), 2254 (w), 2219 (w), 1254 (s) cm^{-1}; UV−vis (ground solid) very broad absorption $\lambda_m = 510$ nm.

X-ray Crystallography of 1ao/TCNE Complex. A yellow prism crystal of $C_{34}H_{44}N_8O_2$ having approximate dimensions of 0.50 × 0.50 × 0.50 mm was mounted on a glass fiber and fixed in a goniometer head on the X-ray diffractometer. Cell constants and an orientation matrix for data collection, obtained from a least-squares refinement using the setting angles of 25 carefully centered reflections in the range $55.1 < 2\theta < 71.7°$, corresponded to a monoclinic cell with dimensions $a = 6.284(2)$ Å, $b = 20.749(3)$ Å, $c = 25.530(4)$ Å, $\alpha = 90.000°$, $\beta = 92.00(2)°$, $\gamma = 90.000°$, $V = 3327(1)$ Å^3. For $Z = 4$ and FW = 596.77, the calculated density is 1.191 g/cm^3.

Based on the systematic absences of hkl ($h + k \neq 2n$), packing considerations, a statistical analysis of intensity distribution, and the successful solution and refinement of the structure, the space group was determined to be $P2_1/c$ (No. 14). These data were collected at a temperature of 20 ± 1 °C using the ω-2θ scan technique to a maximum 2θ value of 120.2°. ω scans of several intense reflections, made prior to data collection, had an average width at half-height of 0.28° with a take off angle of 6.0°. Scans of (1.42 + 0.30 tan θ)° were made at a speed of 8.0°/min (in ω). The weak reflections ($I < 10.0\sigma(I)$) were rescanned (maximum of five rescans), and the counts were accumulated to assure good counting statistics. Stationary background counts were recorded on each side of the reflection. The ratio of peak counting time to background counting time was 2:1. The diameter of the incident beam collimator was 1.0 mm, and the crystal to detector distance was 400.0 mm. A total of 5104 unique reflections were measured, and the final data:parameter ratio was 4.33 with $R = 0.085$, $R_w = 0.096$, and GOF = 3.22.

X-ray Crystallography of 1ado/TCNE Complex. A purple prism crystal of $C_{20}H_{22}N_6O_2$ having approximate dimensions of 0.40 × 0.40 × 0.45 mm was mounted on a glass fiber. Cell constants and an orientation matrix for data collection, obtained from a least-squares refinement using the setting angles of 25 carefully centered reflections in the range $87.1 < 2\theta < 89.5°$, corresponded to a triclinic cell with dimensions $a = 9.204(9)$ Å, $b = 9.703(9)$ Å, $c = 6.243(6)$ Å, $\alpha = 99.711(8)°$, $\beta = 106.76(7)°$, $\gamma = 106.490(7)°$; $V = 492.46(9)$ Å^3. For $Z = 1$ and FW = 378.43, the calculated density is 1.276 g/cm^3.

Based on the systematic absences of hkl ($h + k \neq 2n$),

Table 5. Data from a 1ao/TCNE Temperature Study in CH_2Cl_2 in Which [1ao] = 0.0237 M and [TCNE] = 0.0113 M[a]

temp (K)	$A_{344-800}$, K_f ($\epsilon = 341$)	$A_{364-800}$, K_f ($\epsilon = 673$)	$A_{394-800}$, K_f ($\epsilon = 303$)	$A_{410-800}$, K_f ($\epsilon = 167$)
306.8	0.2245, 2.68	0.2279, 1.32	0.1653, 2.18	0.1132, 2.76
299.9	0.2310, 2.76	0.2329, 1.35	0.1782, 2.37	0.1269, 3.13
286.7	0.2633, 3.19	0.2803, 1.64	0.2192, 2.97	0.1551, 3.92
276.5	0.2789, 3.40	0.3028, 1.78	0.2429, 3.32	0.1728, 4.43
267.8	0.3166, 3.92	0.3455, 2.05	0.2867, 4.00	0.2109, 5.59
$\Delta H°$ (kcal/mol)	−1.57	−1.88	−2.50	−2.82
$\Delta S°$ [cal/(mol K)]	−3.19	−5.62	−6.62	−7.16
r^2	0.980	0.985	0.993	0.988

[a] Data used to calculate values for entry 1, Table 1.

Table 6. Data from a 1ado/TCNE Temperature Study in CH_2Cl_2 in Which [1ado] = 0.0200 M and [TCNE] = 0.0117 M[a]

temp (K)	$A_{500-800}$, K_f ($\epsilon = 3066$)	$A_{520-800}$, K_f ($\epsilon = 1691$)	$A_{540-800}$, K_f ($\epsilon = 3418$)	$A_{550-800}$, K_f (ϵ= 3102)
296.4	0.1394, 0.195	0.1608, 0.411	0.1698, 0.213	0.1693, 0.235
285.8	0.1544, 0.216	0.1774, 0.454	0.1877, 0.236	0.1877, 0.260
274.3	0.1709, 0.240	0.1967, 0.504	0.2085, 0.262	0.2082, 0.289
261.0	0.1888, 0.265	0.2152, 0.552	0.2261, 0.285	0.2257, 0.313
252.4	0.2043, 0.287	0.2338, 0.601	0.2469, 0.311	0.2467, 0.343
$\Delta H°$ (kcal/mol)	−1.28	−1.26	−1.24	−1.24
$\Delta S°$ [cal/(mol K)]	−7.53	−5.97	−7.20	−7.03
r^2	0.996	0.995	0.992	0.991

[a] Data used to calculate values for entry 3, Table 1.

packing considerations, a statistical analysis of intensity distribution, and the successful solution and refinement of the structure, the space group was determined to be $P\bar{1}$ (No. 2). These data were collected at a temperature of 20 ± 1 °C using the ω-2θ scan technique to a maximum 2θ value of 119.9°. ω scans of several intense reflections, made prior to data collection, had an average width at half-height of 0.30° with a take off angle of 6.0°. Scans of $(1.21 + 0.30 \tan \theta)$° were made at a speed of 8.0°/min (in ω). The weak reflections ($I < 10.0\sigma(I)$) were rescanned (maximum of five rescans), and the counts were accumulated to assure good counting statistics. Stationary background counts were recorded on each side of the reflection. The ratio of peak counting time to background counting time was 2:1. The diameter of the incident beam collimator was 1.0 mm, and the crystal to detector distance was 400.0 mm. A total of 1161 unique reflections were measured, and the final data:parameter ratio was 6.48 with $R = 0.054$, $R_w = 0.074$, and GOF = 3.31.

Calculations. Semiempirical PM3 calculations[23] of both *t*-NH(O)NH(O) and *t*-NMe(O)NMe(O) dyad and triad complexes of TCNE were performed using the keyword "precise" to facilitate full optimization of the structures (within imposed constraints as given in the text). Methylated and unmethylated donors gave quite similar geometries.

Acknowledgment. We gratefully acknowledge support of this work by the NSF (CHE-9200144). The X-ray diffractometer facility used for crystal structure determinations was also made possible by funding from the NSF (CHE-8908065).

Supporting Information Available: Spectroscopic data for the determination of Table 1 complexation constants (4 pages). This material is contained in libraries on microfiche, immediately follows this article in the microfilm version of the journal, and can be ordered from the ACS; see any current masthead page for ordering information.

JO960998+